NATIONAL AERONAUTICS AND SPACE ADMINISTRATION

MSC INTERNAL NOTE NO. 68-FM-244

October 3, 1968

GUIDANCE ANALYSIS OF AERODYNAMIC BRAKING INTO ORBIT AROUND MARS

Advanced Mission Design Branch

MISSION PLANNING AND ANALYSIS DIVISION

MANNED SPACECRAFT CENTER
HOUSTON, TEXAS

MSC INTERNAL NOTE NO. 68-FM-244

GUIDANCE ANALYSIS OF AERODYNAMIC BRAKING INTO ORBIT AROUND MARS

By Benjamine J. Garland
Advanced Mission Design Branch

October 3, 1968

MISSION PLANNING AND ANALYSIS DIVISION
NATIONAL AERONAUTICS AND SPACE ADMINISTRATION
MANNED SPACECRAFT CENTER
HOUSTON, TEXAS

Approved: Jack Funk
Jack Funk, Chief
Advanced Mission Design Branch

Approved: J. P. Mayer
John P. Mayer, Chief
Mission Planning and Analysis Division

CONTENTS

FIGURES

GUIDANCE ANALYSIS OF AERODYNAMIC BRAKING INTO ORBIT AROUND MARS

By Benjamine J. Garland

SUMMARY

A guidance system was developed to control a spacecraft during an aerodynamic braking maneuver. The guidance equations attempt to control the apoapsis altitude and inclination of the trajectory after the spacecraft skips from the atmosphere by rolling the spacecraft. A propulsion system is required to change the skip trajectory to the target orbit.

This guidance system was used to evaluate the feasibility of using aerodynamic braking for entry speeds between 17 000 fps and 20 000 fps. The assumed spacecraft had a lift-to-drag (L/D) ratio of 0.5 and a ballistic coefficient of 120 psf. The use of aerodynamic braking appears to be feasible provided that an accurate model of the Martian atmosphere is available.

INTRODUCTION

The use of aerodynamic braking to achieve the capture of a spacecraft by the atmosphere of a planet has been shown to offer advantages over propulsive braking by many studies (refs. 1 through 9). The aerodynamic braking maneuver may be used for either a direct descent to the surface or just to decelerate the spacecraft to allow its capture after it skips from the atmosphere. During the first skip the propulsion system must be used to raise the periapsis altitude of the orbit above the planetary atmosphere if an orbit is to be established. It may be necessary to use the propulsion system a second time to adjust the apoapsis altitude.

The depth of the corridor available for aerodynamic braking at Mars was studied by analytic means in references 1 and 2. The results indicate that a spacecraft could be guided to the available corridor with comparative ease. The trajectory of the spacecraft through the atmosphere was considered in references 3 and 4, although the major emphasis of reference 3 was placed on aerodynamic braking maneuvers at Earth. The problem of

aerodynamic braking at Mars was examined in reference 4 using a two-dimensional trajectory simulation that employed a calculus-of-variation procedure for trajectory optimization. The optimum trajectory was found to require either full positive or full negative lift and an instantaneous reversal of the lift vector. An alternate type of trajectory containing a constant altitude segment was considered because a real guidance and control system is not capable of following the optimum trajectory. It was found that the cost of the alternate trajectory could be kept close to the cost of the optimum trajectory if the target orbit was chosen judiciously.

The models of the Martian atmosphere used in references 1 through 4 are now believed to be incorrect. For example, the density of the atmospheric model used in reference 4 is approximately two orders of magnitude greater than the density of the mean atmosphere proposed in reference 10. The atmospheric models used in references 5 and 6 are basically the same as the proposed model.

Some of the problems of the automatic control system necessary to achieve aerodynamic braking at Mars were discussed in reference 11. The control system used a fast-time prediction guidance method, such as discussed in reference 12 to predict the proper controls. In addition, some results of simulations of manual backup control were presented. Unfortunately, this study was performed before the present model of the Martian atmosphere was obtained.

A comprehensive study of the use of aerodynamic braking to achieve planetary capture of the spacecraft has been reported in reference 9. The initial mass in orbit at Earth for a spacecraft employing aerodynamic braking was compared to that of a spacecraft employing only propulsive braking. The initial mass of each spacecraft was reduced significantly by increasing the eccentricity of the orbit and are comparable when the eccentricity is 0.7. The aerodynamic braking spacecraft had an L/D of 1.0 and a ballistic coefficient of 1000 psf.

The initial mass in Earth orbit may be reduced further by the procedure suggested in reference 13. This procedure uses aerodynamic braking for the spacecraft which will be used to descend to the surface of the planet but uses propulsive braking for the main spacecraft. The crew remains aboard the main spacecraft while the unmanned lander spacecraft uses aerodynamic braking to achieve capture.

A guidance system for controlling the spacecraft during the aerodynamic braking maneuver has been developed. This guidance system uses a closed-form prediction technique rather than a fast-time prediction technique such as that used in reference 11. The guidance equations attempt to control both the apoapsis altitude of the exit trajectory and the

inclination of the trajectory plane. This guidance system was used to study the feasibility to perform the aerodynamic braking maneuver with the landing spacecraft discussed in references 9 and 13. The landing spacecraft is capable of achieving an L/D of 0.5 and has a ballistic coefficient of 120 psf. The models of the Martian atmosphere proposed in reference 9 were used and the velocity of the spacecraft at entry was assumed to be between 17 000 fps and 20 000 fps. Entry velocities in this range can be obtained with round-trip missions which last approximately 1000 days and remain at Mars for approximately 450 days (ref. 7).

METHOD

Description of Maneuvers to Establish Orbit

The sequence of maneuvers used to establish the orbit is shown in figure 1. The spacecraft approaches the planet along a hyperbolic path which must intersect the atmosphere with certain limits known as the entry corridor. The limits of the corridor may be specified either by the vacuum periapsis altitude of the hyperbolic trajectory or by the flight-path angle at some arbitrary altitude. The basic purpose of the atmospheric phase is to change the path of the spacecraft so that it exits from the atmosphere along a trajectory having an apoapsis altitude equal to that of the target orbit. The velocity of the spacecraft must be increased at the apoapsis of the exit trajectory in order to raise the periapsis altitude to the desired value. Since the exit trajectory will not achieve the proper apoapsis altitude, the spacecraft's velocity is changed a second time at the periapsis of the intermediate orbit. A convenient measure of the performance of the guidance system and spacecraft combination is the total velocity change required to achieve the target orbit.

A more detailed description of the atmospheric phase is shown in figure 2. The beginning and end of this phase are impossible to define except by some arbitrary means such as the magnitude of the acceleration caused by the aerodynamic force. The atmospheric phase is divided into three subdivisions by the guidance system. These subdivisions are the transition to a constant altitude path, the constant altitude path, and the exit.

Description of Guidance System

Some of the quantities which are used in the guidance equations are shown in figure 3. These quantities are commonly used in the study of entry trajectories.

The characteristics of the spacecraft must be considered in the development of the guidance equations. In this case, the entry vehicle was assumed to be a body of revolution capable of producing a constant ratio of L/D. The trajectory of the spacecraft can be controlled only by varying the roll angle.

The guidance system is a closed-form prediction method instead of a fast-time prediction method such as is used in reference 11. The differences between the two methods are discussed in detail in reference 12. The fast-time prediction method requires the rapid numerical solution of the differential equations of motion by the onboard computer in order to determine the possible future trajectories. The closed-form prediction method uses approximate analytic solutions to the equations of motion instead of integrating them by numerical methods.

The basic arrangement of the guidance logic is shown in figure 4. The guidance commands are based on the changes in the velocity measured by the inertial measurement unit (IMU). The navigation section uses the measurements of the IMU to obtain the position and velocity of the spacecraft. The navigation equations are basically the same as those used for Project Apollo (ref. 14) and are used in each cycle of the computer.

The mode selector serves only to direct the computations to the correct phase. The roll angle of the spacecraft is held constant as long as the initial phase continues. The initial phase is terminated whenever the measured acceleration along the velocity vector exceeds 3.2 ft/sec^2 (0.1 g_e, where g_e is the gravitational acceleration of the Earth).

The purpose of the next phase is to steer the spacecraft onto a constant altitude path. The velocity of the spacecraft and the atmospheric density at the beginning of the constant altitude phase depend upon the arbitrary value of L/D at this point. The guidance equations for the transition phase are based on the method of reference 15 although the derived equations are different. The development of these equations is discussed in the appendix. The required value of L/D is given by equation (A9) of this appendix. The commanded roll angle, ϕ_c, is

$$\phi_c = \cos^{-1}\left[\left(\frac{L}{D}\right)_c \Big/ \left(\frac{L}{D}\right)_m\right] \qquad (1)$$

where $(L/D)_m$ is the maximum L/D and $(L/D)_c$ is the command L/D.

The constant altitude allows the spacecraft to decelerate until the proper apoapsis altitude can be reached. Therefore, a portion of the

computations for the exit phase must be performed each cycle although the spacecraft is still being guided along a constant altitude path. The constant altitude phase continues until the target apoapsis altitude can be reached by using a constant value of L/D less than some specified value. The L/D required to maintain a constant altitude path is given by equation (A14) of the appendix.

The exit phase guidance equations are based on the second-order solution to the equations of motion presented in references 16 and 17. The use of this solution is discussed in the appendix. The second-order solution is used to calculate the apoapsis altitude achieved by using a constant value of the L/D. A Newton-Raphson iteration scheme is used to determine the correct value of the L/D. This value was used to steer the spacecraft originally, but better results were obtained if the roll angle was based on the following equation:

$$\left(\frac{L}{D}\right)_c = k_1 \left(\frac{L}{D}\right) + k_2 \left[\left(\frac{L}{D}\right) - \left(\frac{L}{D}\right)_{REF}\right] \qquad (2)$$

k_1 and k_2 are the gains. The value of L/D obtained from the previous cycle through the equations is used for L/D_{REF}. The exit phase ends whenever the measured acceleration along the velocity vector decreases below 3.2 ft/sec^2.

The inclination of the orbit is controlled by the direction of the roll angle. It is assumed that the change in the inclination of the orbit is approximated by the change in the spacecraft's heading. The approximate change in heading is given in reference 18. The estimate of the change in inclination during the atmospheric phase is compared to the desired inclination in order to determine the direction of roll.

NUMERICAL APPLICATION AND RESULTS

A four-degree-of-freedom digital trajectory program was used to evaluate the performance of the combined guidance system and spacecraft. The trajectory program assumed a spherical rotating planet. The physical properties presented in reference 19 and the atmospheric models of reference 10 were used in the study. The nominal characteristics of the spacecraft and control systems are listed on the following page.

L/D	0.5
$W/C_D s$, psf	120
Maximum roll rate, deg/sec	±20
Roll acceleration, deg/sec^2	±10
Roll deadband, deg	±4

The control system characteristics are those of the Apollo command module. The variation of the atmospheric density with altitude is presented in figure 5 for the high, mean, and low density atmospheres.

An initial altitude of 300 000 ft was used for all trajectories, and two initial velocities (17 000 and 20 000 fps) were investigated. Either the periapsis altitude of the approach trajectory or the flight-path angle at the initial altitude is required to completely specify the entry conditions. Two target orbits were considered in the study. The apoapsis altitude was either 1000 n. mi. or 10 000 n. mi. whereas the periapsis altitude was 100 n. mi. for both orbits. The eccentricities of the orbits are 0.188 and 0.718, respectively. The total velocity change (ΔV_T) necessary to establish the target orbit is used as a measure of performance of the guidance and spacecraft combination.

The altitude, velocity, and flight-path angle of two typical entry trajectories are presented in figure 6 as functions of time. The entry velocity is 20 000 fps, and the flight-path angle is -8.2° for both trajectories. The basic difference between the two trajectories is that the apoapsis altitudes of the target orbits are 1000 n. mi. and 10 000 n. mi. The two trajectories are identical until 146 seconds when the exit phase of the 10 000-n. mi. apoapsis altitude trajectory begins. The velocity is 16 804 fps at this time. The constant altitude phase continues for another 90 seconds if the target apoapsis altitude is lowered to 1000 n. mi. During this 90 seconds, the velocity of the spacecraft decreases to 14 165 fps. The exit conditions for the two trajectories are listed in the following table.

Apoapsis altitude of target orbit, n. mi.	10 000	1 000
Exit altitude, ft	214 394	201 358
Exit velocity, fps	15 185	12 664
Exit flight-path angle, deg	4.83	3.96

These exit conditions result in actual apoapsis altitudes of 10 438 n. mi. and 1023 n. mi. Total velocity changes of 80.3 fps and 142.7 fps are required to achieve the proper orbits.

In the case of the 10 000-n. mi. target apoapsis altitude trajectory, a change of 1° in the flight-path angle at exit will cause a change of 6 n. mi. in the apoapsis altitude while a change of 1 fps in the velocity at exit will cause a change of 13 n. mi. in the apoapsis altitude. If the target apoapsis altitude is 1000 n. mi., a 1° change in the flight-path angle at exit will result in a change in the apoapsis altitude of 12 n. mi. However, the apoapsis altitude will be changed by only 1.1 n. mi. if the velocity at exit is changed 1 fps. The errors in the velocity at exit probably will be greater for the trajectory which spends the greatest amount of time in the atmosphere.

The ΔV_T required to establish a 10 000-n. mi. apoapsis altitude orbit is presented in figure 7 as a function of the flight-path angle at entry (γ_{en}) and as a function of the periapsis altitude of the approach path ($h_{p,\ vac}$). The entry velocity (V_{en}) is 20 000 fps. Although the three atmospheric models were used, the guidance was based upon the parameters of the mean atmosphere. The symbols on the figures represent results of individual trajectories while the solid lines are intended to show general trends only. The results for the mean density atmosphere show a distinct region of low ΔV_T. This region of low ΔV_T can be described as the entry corridor for the aerodynamic braking maneuver. The ΔV_T is between 60 and 87 fps if γ_{en} is between -9.0° and -7.6° ($14.5 \leq h_{p,\ vac} \leq 24.5$). The ΔV_T increases sharply outside of the corridor. The ΔV_T for the low density also exhibits a distinct corridor although the ΔV_T is approximately 100 fps higher than that required for the mean density atmosphere. The ΔV_T required for the high density atmosphere is comparable to that required for the low density atmosphere. This figure was based on the assumption that the maximum density atmosphere and the low density atmosphere are the maximum expected deviations from the mean density atmosphere and the correct density will not be known.

The definition of the entry corridor used in this report is more restrictive than the definition used in reference 9. That reference defined the bottom of the corridor by the full positive-lift trajectory which just reached the minimum allowable altitude and the top of the corridor was defined by the full negative-lift trajectory which resulted in an overshoot. The entry corridor defined in this manner is a function of the entry velocity, the physical properties of the spacecraft, and

the atmosphere of the planet. This report defines an entry corridor which also depends upon the target apoapsis altitude and the guidance and control system.

The cases presented in figure 8 are the same as those in figure 7 except that the guidance uses the correct atmospheric parameters. There is a distinct corridor for each atmospheric model and the ΔV_T in the corridors is between 45 and 100 fps. The depth of the corridor is 2.2° (13.2 n. mi.) for the high density atmosphere, 1.4° (10.0 n. mi.) for the mean density atmosphere, and 1.2° (9.3 n. mi.) for the low density atmosphere. The center of each corridor is shifted so that the corridors do not all overlap.

The effect of variations in the ballistic coefficient (W/C_DS) is shown in figure 9. Variations of ±20 psf had little effect upon the entry corridor or the ΔV_T required within the corridor although the guidance was based on the nominal ballistic coefficient of 120 psf. The effect was the same for all three atmospheres. The analytic results of reference 1 indicate that the depth of the corridors should not be affected by changes in the ballistic coefficient but that the center of the corridor should be shifted as the ballistic coefficient is changed.

The effect of reducing the L/D to 0.4 is shown in figure 10. The guidance equations used the nominal L/D of 0.5. This reduction in L/D caused a decrease in the depth of the corridor but did not shift the center of the corridor. The depth of the corridor was reduced to 1.6° (9.6 n. mi.) for the high density atmosphere and 0.6° (4.5 n. mi.) for the low density atmosphere. This is a reduction of approximately 27 percent for the high density atmosphere and 52 percent for the low density atmosphere.

The target orbit in figures 7 to 10 has an apoapsis altitude of 10 000 n. mi. and a periapsis altitude of 100 n. mi. The ΔV_T required to establish a 1000-n. mi. apoapsis altitude orbit is given in figure 11. In general, the ΔV_T is increased approximately 100 fps above that required to achieve a 10 000-n. mi. apoapsis altitude orbit. The top of the corridor occurs at approximately the same point, but the bottom of the corridor is not distinctive. If the flight-path angle at entry is decreased below a certain value, the ΔV_T will begin to increase but not as rapidly as it did for the higher apoapsis altitude orbit. Also, there is considerable fluctuation in the required ΔV_T.

The entry velocity of the spacecraft is not likely to be less than 17 000 fps since this is approximately 4 percent greater than the escape

velocity at 300 000 ft. The ΔV_T required to establish a 10 000-n. mi. apoapsis altitude when the entry velocity is 17 000 fps is shown in figure 12. A ΔV_T of 500 fps is necessary to maintain a corridor depth of 0.8° (6.7 n. mi.) for the low density atmosphere. The mean and high density atmospheres require higher values of ΔV_T. The ΔV_T decreased to approximately 100 fps for the low density and mean density atmospheres before increasing rapidly. This rapid fluctuation can be explained by examining the next figure.

The apoapsis altitude of the exit trajectory is presented in figure 13 for the same condition used in the previous figure. The apoapsis altitude is almost constant over some range of entry angles for each of the atmospheric models. This apoapsis altitude is not the nominal value of 10 000 n. mi. but varies between 6700 n. mi. for the low density atmosphere and 4000 n. mi. for the high density atmosphere. If the entry angle is decreased, the apoapsis altitude decreases until eventually the spacecraft will not escape the atmosphere of the planet. If the entry angle is increased, the apoapsis altitude of the exit trajectory will increase without limit. The minimum values of ΔV_T shown in figure 12 for the low and mean density atmospheres occur when the apoapsis altitude of the exit trajectory is equal to the apoapsis altitude of the target orbit. The ΔV_T for the high density atmosphere should exhibit the same trends.

The results presented in figure 13 indicate that there is a maximum value which should be used for the apoapsis altitude of the target orbit. This maximum value corresponds to the nearly constant valued portions of the curves in figure 13. Since the correct model of the atmosphere is not known, the maximum apoapsis altitude is given by the high density model. The maximum apoapsis altitude of the target orbit is given as a function of the entry velocity in figure 14. It can be seen that the entry velocity must be above 18 850 fps if the target apoapsis altitude is 10 000 n. mi.

The effect of reducing the target apoapsis altitude to 1000 n. mi. when the entry velocity is 17 000 fps is shown in figure 15. Now, there is a definite entry corridor for all three atmospheres. The ΔV_T within the corridor is between 120 and 170 fps. The depth of the corridor is 2.2° (14.5 n. mi.) for the high density atmosphere and 1.0° (8.7 n. mi.) for the low density atmosphere. The depth of the corridors and the ΔV_T within the ocrridors are approximately the same for an entry velocity of 17 000 fps as for an entry velocity of 20 000 fps. The major difference is that the center of the corridor has been raised by the decrease in the entry velocity.

All of the trajectories considered in this study were in the equatorial plane of Mars initially. The entry guidance attempted to keep the exit trajectory in the equatorial plane also. The inclination of the exit trajectory was less than 0.2° for all of the cases. The maximum controllable change in the inclination is approximately 2.0°. The minimum altitude of trajectories within the entry corridors was never less than 50 000 ft and the maximum acceleration was less than 2.5 g_e.

An analysis of the navigation and guidance of a Mars probe launched from a manned spacecraft was reported in reference 19. Although the results of reference 19 are not directly applicable to the present study, the dispersions in the entry angle should be approximately the same magnitude. The standard deviation in the entry angle was found to be between 0.13° and 0.21°. If the dispersion in the entry angle is as low as 0.13° and the L/D is 0.5, the probability that the spacecraft will miss the corridor is very small. The probability of achieving the corridor is 97.9 percent if the low density atmosphere occurs and the L/D is 0.4.

The centers of the low and high density atmospheres are displaced from the center of the mean density atmosphere by approximately 0.8°. This displacement of the corridors insures that a single value of the entry angle cannot be selected on the basis of the present knowledge of the Martian atmosphere. It is possible that this problem may be solved by launching an atmospheric probe from the main spacecraft so that the probe arrives at the planet before the main spacecraft and the aerobraking spacecraft. An approximation of the atmosphere is made on the basis of data received from the probe, and the aerodynamic braking spacecraft is aimed at the correct entry angle. The total velocity increment necessary to change the entry angle by ±1° is presented in figure 16 as a function of the time remaining before entry. The entry velocity was 17 000 fps and the entry angle was -7.1°. If the trajectory is corrected 10 minutes before the time of entry, a velocity change of less than 59 fps is required to change the entry angle by ±1°. The velocity change decreases to less than 22 fps when the connection takes place 30 minutes before entry. The results were approximately the same when the entry velocity was 20 000 fps and the nominal entry angle is -8.2°.

CONCLUDING REMARKS

The feasibility of achieving a specified orbit about Mars by using aerodynamic braking depends upon the knowledge of the environment, the physical properties of the spacecraft, and the properties of the target orbit. An orbit cannot be successfully established unless the approach trajectory is targeted to the center of the corridor for the correct

atmosphere. If the correction is made 30 minutes before the time of entry, a velocity change of less than 22 fps is required. The total velocity change required to achieve an orbit with an apoapsis altitude of 10 000 n. mi. and a periapsis altitude of 100 n. mi. is between 45 and 100 fps if the entry speed is 20 000 fps and the L/D is 0.5. A decrease in either the entry velocity or the L/D may require that the apoapsis altitude be decreased. The required total velocity change is increased to between 120 and 170 fps if the apoapsis altitude of the target orbit is decreased to 1000 n. mi.

The effect of errors on the performance of the guidance system and the spacecraft was not considered. The presence of any errors will cause a reduction in the corridor and will increase the difficulty of achieving the target orbit. The sequence of maneuvers required to establish the target orbit suggests a procedure to achieve the orbit which most closely approximates the target orbit. The first velocity change raises the periapsis altitude to required value. A second velocity change is required to establish the desired apoapsis altitude. If necessary, the maximum allotted velocity change would be used to move the apoapsis altitude as close to desired value as possible.

APPENDIX

GUIDANCE EQUATIONS

APPENDIX

GUIDANCE EQUATIONS

SYMBOLS

a	acceleration, ft/sec^2
C_D	drag coefficient
e	eccentricity
g	gravitational acceleration of planet, ft/sec^2
h	altitude, ft
K	trajectory constant defined in equation (A17), $ft^4/lb\text{-}sec^2$
k_1, k_2	gains defined in equation (2)
k_3, k_4, k_5	gains defined in equation (A14)
L/D	lift-to-drag ratio
m	mass, $lb\text{-}sec^2/ft$
R	radius of planet, ft
r	radius, ft
S	reference area, ft^2
t	time, sec
V	velocity, fps
W	weight, lb
β	density decay parameter, ft^{-1}

γ	flight-path angle, deg or rad
ΔV_T	total velocity change required to establish target orbit
$\Delta\rho$	change in density, defined by equation (A10), $lb\text{-}sec^2/ft^4$
θ	central angle of the planet, deg or rad
ρ	density of atmosphere, $lb\text{-}sec^2/ft^4$
ϕ	roll angle of spacecraft, deg or rad

Subscripts:

a	apoapsis
c	command
D	drag
e	Earth
en	entry
ex	exit
i	initial
m	maximum
REF	reference
o	constant altitude
p	periapsis
vac	vacuum

TRANSITION TO CONSTANT ALTITUDE

Guidance equations capable of steering the spacecraft to a constant altitude path were presented in reference 13. These equations are based on the assumptions that the velocity is constant and the flight-path angle

is small during this phase. Although these equations were originally developed to use either full positive or negative lift, it is possible to modulate the lift to achieve a smoother transition to the constant altitude path.

The two-dimensional equations of motion of a vehicle moving through the atmosphere of a planet are:

$$\dot{h} = V \sin \gamma \tag{A1}$$

$$\dot{\theta} = \frac{V}{r} \cos \gamma \tag{A2}$$

$$V\dot{\gamma} = \frac{1}{2}\left(\frac{L}{D}\right)\frac{C_D S}{m}\rho V^2 - g \cos \gamma\left(1 - \frac{V^2}{gr}\right) \tag{A3}$$

$$\dot{V} = -\frac{1}{2}\frac{C_D S}{m} V^2 \rho - g \sin \gamma \tag{A4}$$

The atmosphere of the planet is assumed to be isothermal so that the density is an exponential function of the altitude. The density is:

$$\rho = \rho_o \exp(-\beta h) \tag{A5}$$

If V is constant and γ is small during the transition phase, equation (A1) and (A3) become

$$\dot{h} = V\gamma \tag{A6}$$

and

$$\dot{\gamma} = \frac{1}{2}\left(\frac{C_D S}{m\beta}\right)\rho V - \frac{g}{V}\left(1 - \frac{V^2}{gr}\right) \tag{A7}$$

respectively. The time rate of change of ρ is found from equation (A5). After rewriting, $\dot{\rho}$ is

$$\dot{\rho} = -\beta\rho V\gamma \tag{A8}$$

Equation (A7) is divided by (A8) to obtain

$$\frac{d\gamma}{d\rho} = -\frac{\left(\frac{L}{D}\right)\left(\frac{C_D S}{m}\right)}{2\beta\gamma} + \frac{g}{\beta\rho\gamma V^2}\left(1 - \frac{V^2}{gr}\right)$$

After being rearranged, this equation can be integrated between the proper limits and solved for L/D. The resulting equation is

$$L/D = \frac{\beta\gamma_i^2}{\left(\frac{C_D S}{m}\right)\Delta\rho} + \frac{2g}{V^2\left(\frac{C_D S}{m}\right)\Delta\rho}\left(1 - \frac{V^2}{gr}\right)\ln\left(1 + \frac{\Delta\rho}{\rho_i}\right) \quad (A9)$$

where

$$\Delta\rho = \rho_o - \rho_i \quad (A10)$$

If the value of L/D is specified at the beginning of the constant altitude phase, the density along the constant altitude path is

$$\rho_o = \frac{2g}{\left(\frac{L}{D}\right)\left(\frac{C_D S}{m}\right) V^2}\left(1 - \frac{V^2}{gr}\right) \quad (A11)$$

The maximum permissible density is

$$\rho_o = \frac{2a_m}{\left(\frac{C_D S}{m}\right) V^2}$$

The lowest value of ρ_o is used to determine $\Delta\rho$. The value of ρ_i is calculated as

$$\rho_i = \frac{2a_D}{\left(\frac{C_D S}{m}\right) V^2} \quad (A12)$$

CONSTANT ALTITUDE PATH

The L/D required to maintain a constant altitude is found by setting γ and $\dot{\gamma}$ equal to zero and solving equation (A3) to obtain

$$L/D = \frac{g}{a_D}\left(1 - \frac{V^2}{gr}\right) \quad (A13)$$

where the measured acceleration a_D replaces the term

$$\frac{1}{2}\rho V^2 \quad \frac{C_D S}{m}$$

It is necessary to add additional terms to equation (A13) in order to insure the stability of the path. Since the altitude is constant, the acceleration at any time can be related to the acceleration at the beginning of the constant altitude phase. This relationship is

$$a = \frac{V}{V_i} a_{D,\,i}$$

The control equation which is used for the constant altitude phase is

$$(L/D) = \left(1 - \frac{V^2}{gr}\right) \frac{g}{a_D} - k_3 \left[a_D - \left(\frac{V}{V_i}\right)^2 a_{D,\,i}\right] - k_4 \dot{h} - k_5 \ddot{h} \tag{A14}$$

where k_3, k_4, and k_5 are constant gains.

GUIDANCE EQUATIONS FOR EXIT PHASE

A second-order solution to the equations of motion within an atmosphere was presented in reference 14 and extended to trajectories which exit from the atmosphere in reference 15. The flight-path angle was defined to be positive when the altitude is decreasing. In order to be consistent with the rest of the guidance equations, the flight-path angle is redefined to be positive when the altitude is increasing. The second-order solution is

$$\ln\left(\frac{V^2}{V_i^2}\right) = \frac{\left(\frac{C_D S}{m\beta}\right)(\gamma_i - \gamma)}{\frac{1}{2}\left(\frac{C_D S}{m\beta}\right)\left(\frac{L}{D}\right) - \frac{1}{\beta R}\frac{\cos\gamma}{\rho}\left(\frac{R}{\frac{g}{V^2}} - 1\right)} \tag{A15}$$

and

$$\cos\gamma = \cos\gamma_i + (\rho - \rho_i)\left[\frac{1}{2}\left(\frac{L}{D}\right)\frac{C_D S}{m\beta} - \frac{1}{\beta R}\frac{\cos\gamma}{\rho}\left(\frac{R}{\frac{g}{V^2}} - 1\right)\right] \tag{A16}$$

The second-order solution is based on the approximation that the term

$$\frac{1}{\beta R} \frac{\cos \gamma}{\rho} \left(\frac{g^R}{V^2} - 1 \right)$$

remains constant. Loh (ref. 16) emphasizes that although this term remains nearly constant, the individual values of γ, ρ, and V do not remain constant. For convenience, define

$$K = \frac{1}{\beta R} \frac{\cos \gamma}{\rho} \left(\frac{g^R}{V^2} - 1 \right) \tag{A17}$$

so that equations (A15) and (A16) become

$$V = V_i \exp \left\{ \frac{1}{2} \frac{C_D S}{m\beta} (\gamma_i - \gamma) \left[\frac{1}{2} \left(\frac{L}{D} \right) \left(\frac{C_D S}{m\beta} \right) - K \right]^{-1} \right\} \tag{A18}$$

and

$$\cos \gamma = \cos \gamma_i + (\rho - \rho_i) \left[\frac{1}{2} \left(\frac{L}{D} \right) \left(\frac{C_D S}{m\beta} \right) - K \right] \tag{A19}$$

respectively.

The velocity and flight-path angle at exit are obtained by setting ρ equal to zero in equations (A18) and (A19). The altitude at the time of exit is assumed to be the same as the altitude at the beginning of the transition phase. The predicted velocity, flight-path angle, and altitude at exit are used to predict the apoapsis altitude of the exit trajectory. The motion of the spacecraft outside the atmosphere is described by the two-body equations of motion which are discussed sources such as reference 19. The eccentricity of the exit trajectory is

$$e = \left[1 + \left(\frac{R + h_{ex}}{R} \right)^2 \left(\frac{V^2_{ex}}{gR} \right) \left(\frac{V^2_{ex}}{gR} - \frac{2R}{R + h_{ex}} \right) \cos^2 \gamma_{ex} \right]^{\frac{1}{2}} \tag{A20}$$

and the apoapsis altitude is

$$h_a = \left[\frac{\cos^2 \gamma_{ex}}{(1 - e)} \left(\frac{R + h_{ex}}{R} \right)^2 \frac{V^2_{ex}}{gR} - 1 \right] R \tag{A21}$$

An examination of equations (A18) through (A21) indicate that the apoapsis altitude is a function of L/D which can be controlled by the roll angle of the spacecraft. The value of L/D necessary to achieve the desired apoapsis altitude is found using a Newton-Raphson iteration scheme.

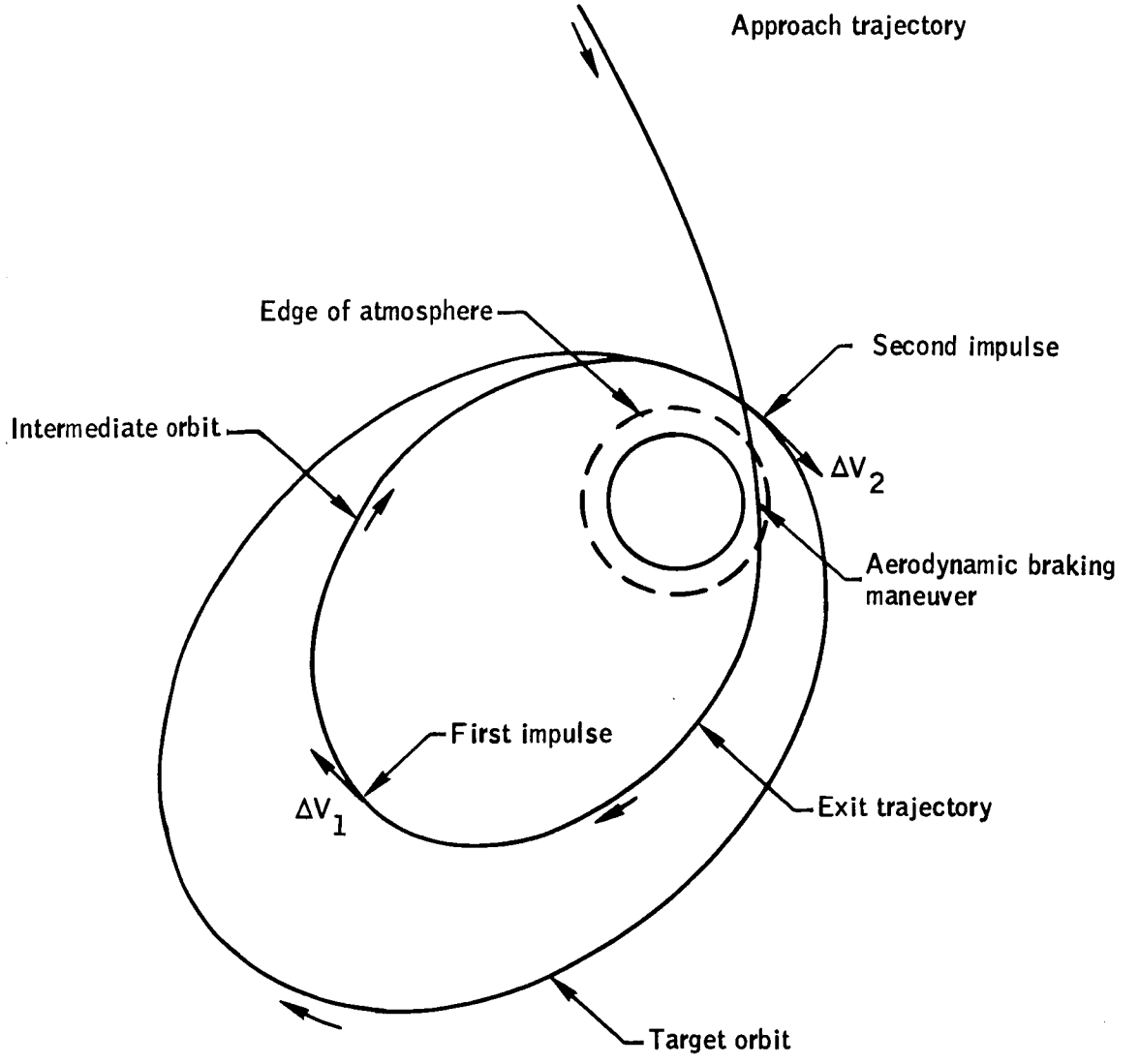

Figure 1.- Sequence of maneuvers necessary to establish target orbit.

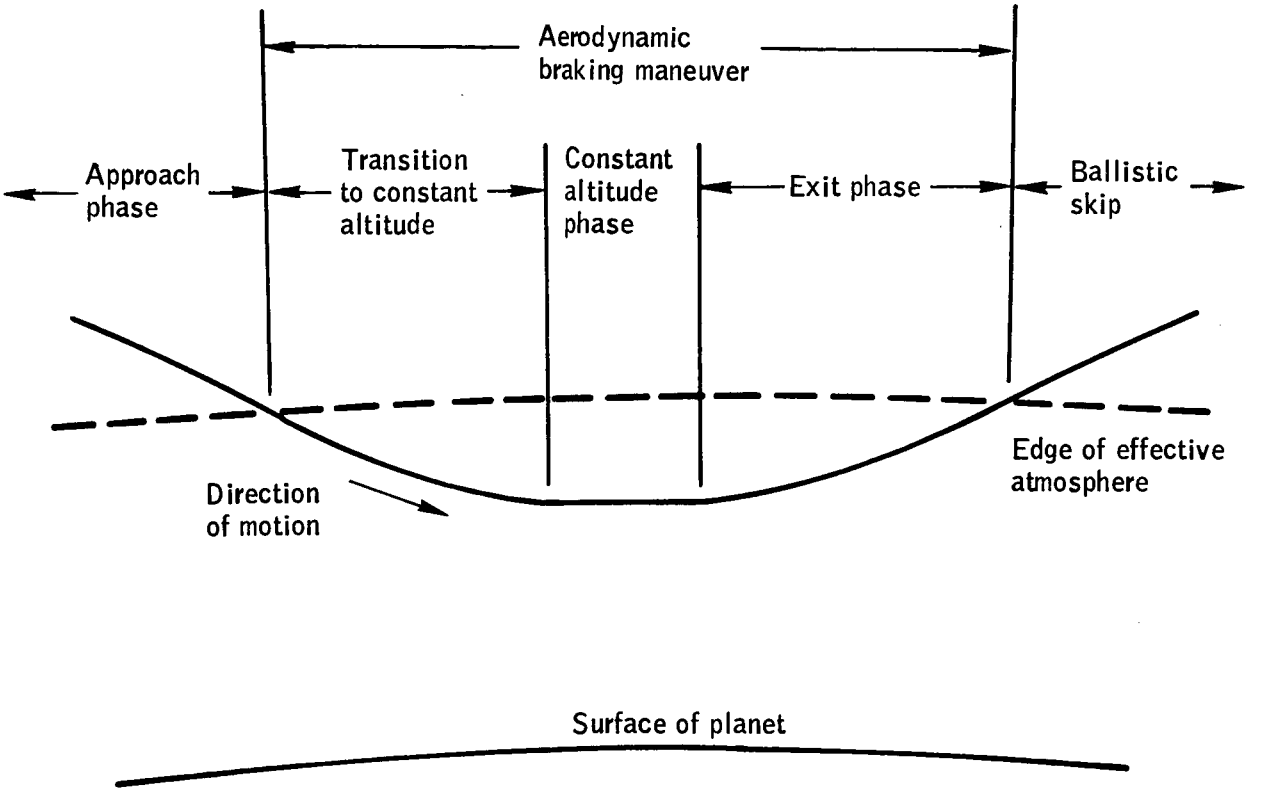

Figure 2.- Phases of aerodynamic braking maneuver.

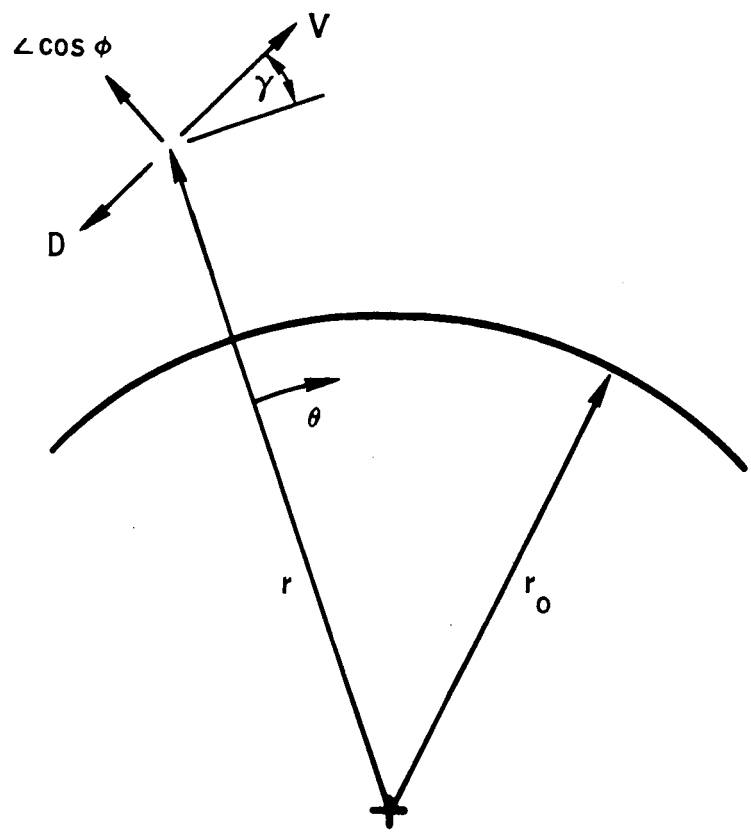

Figure 3.- Quantities used in equations of motion.

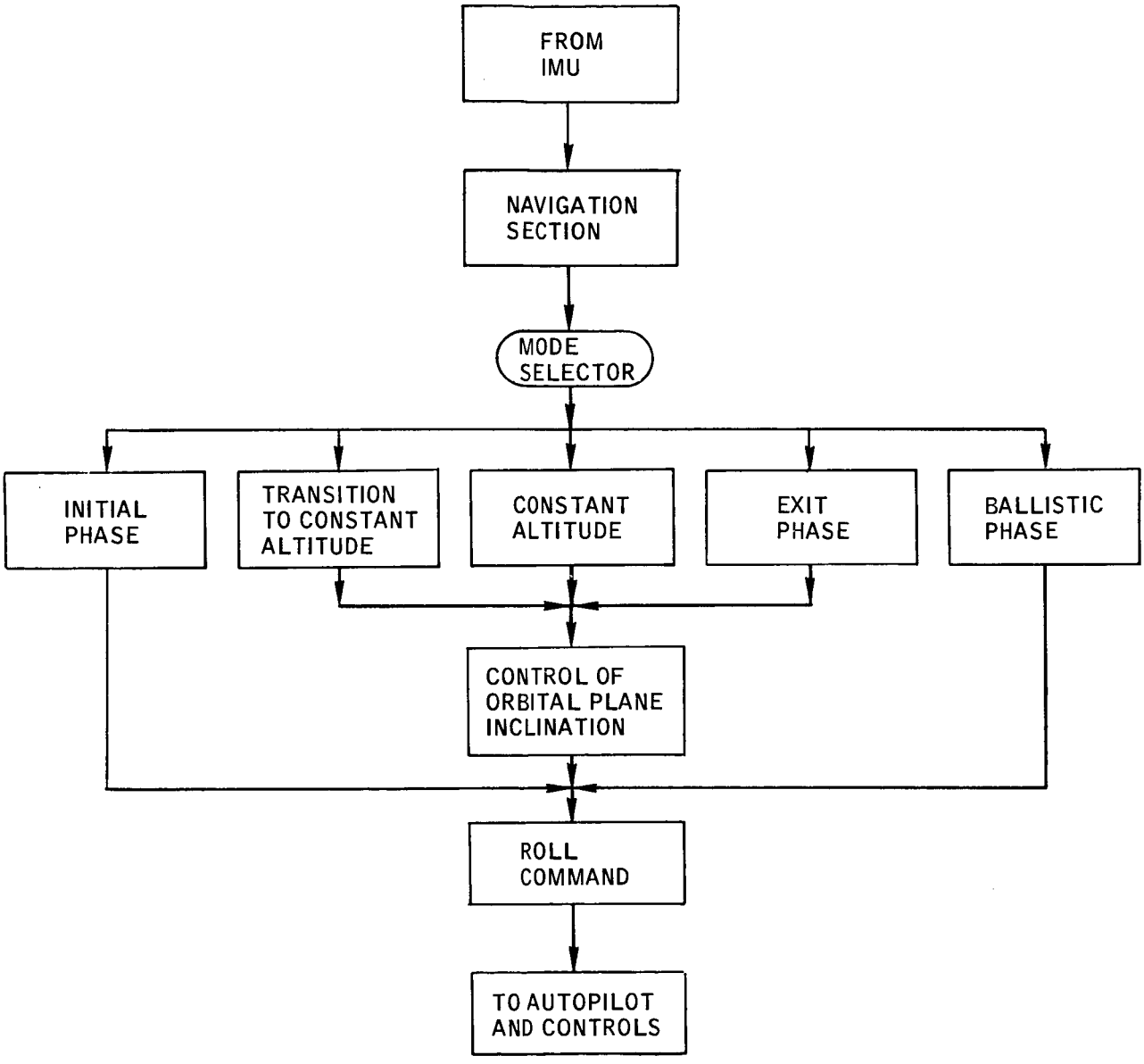

Figure 4.- Basic logic of guidance.

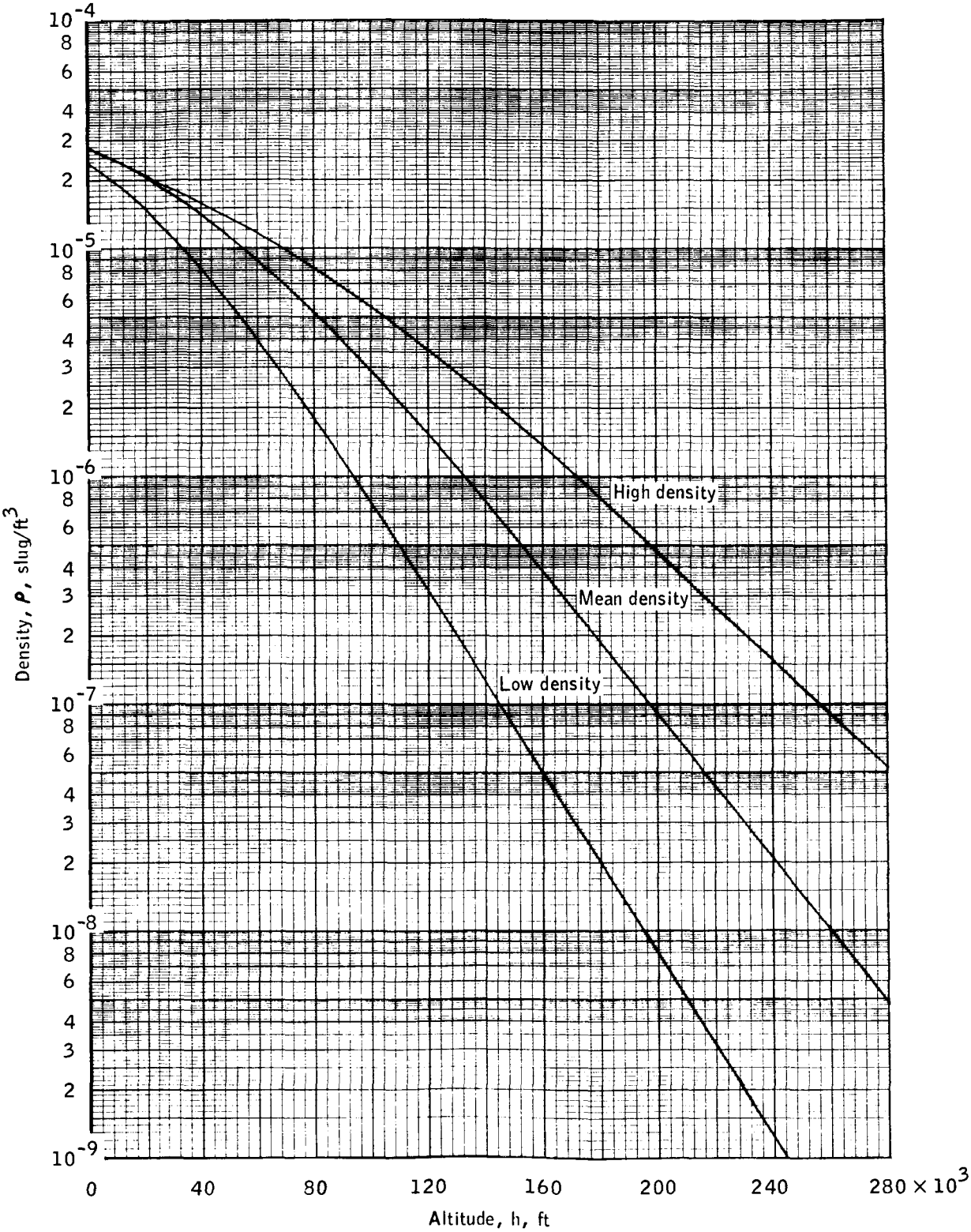

Figure 5.- Atmospheric models used in study.

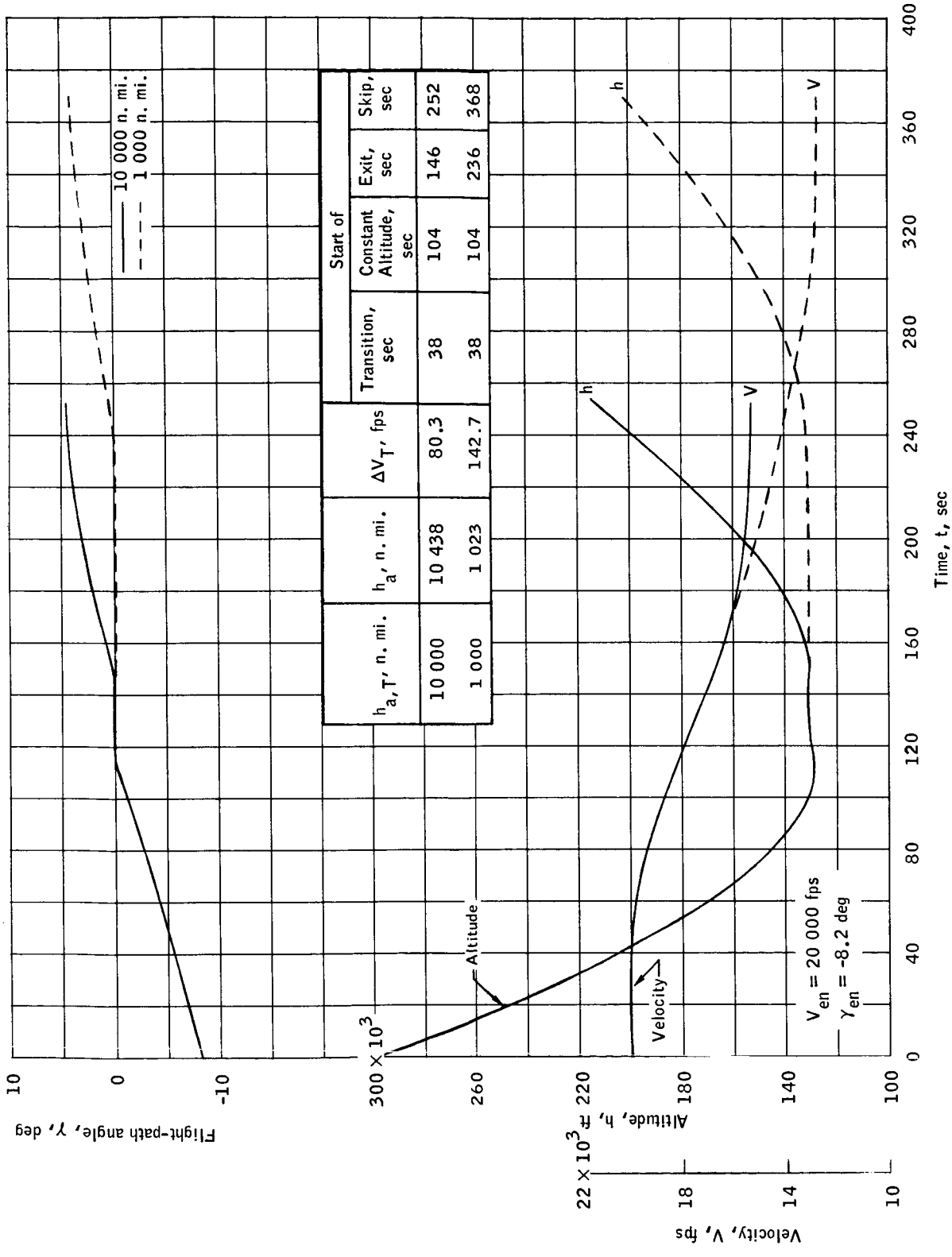

Figure 6.- Time histories of altitude, velocity, and flight-path angle for two typical trajectories.

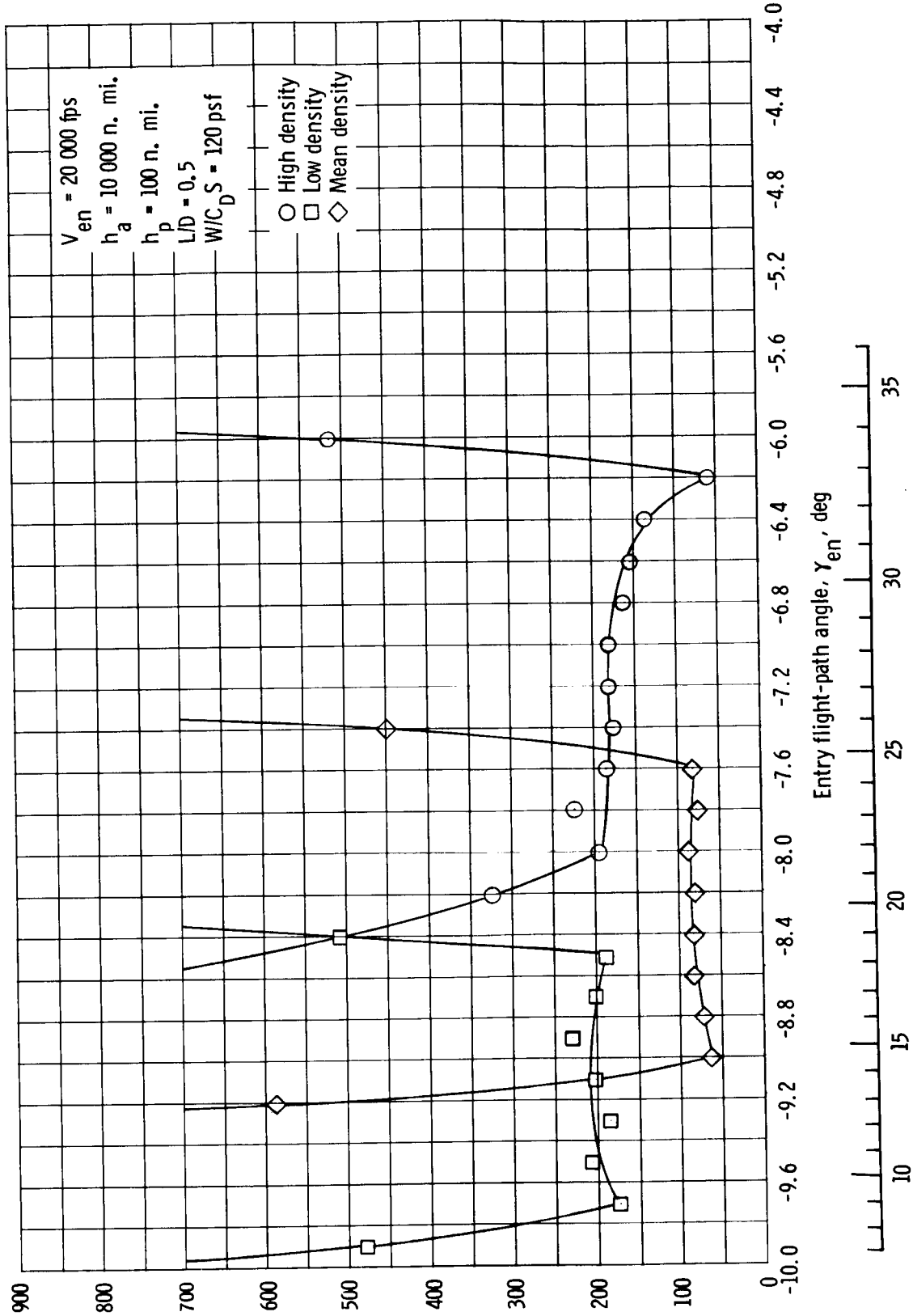

Figure 7.- Total velocity change required to establish target orbit if the guidance is based on parameters of mean density atmosphere.

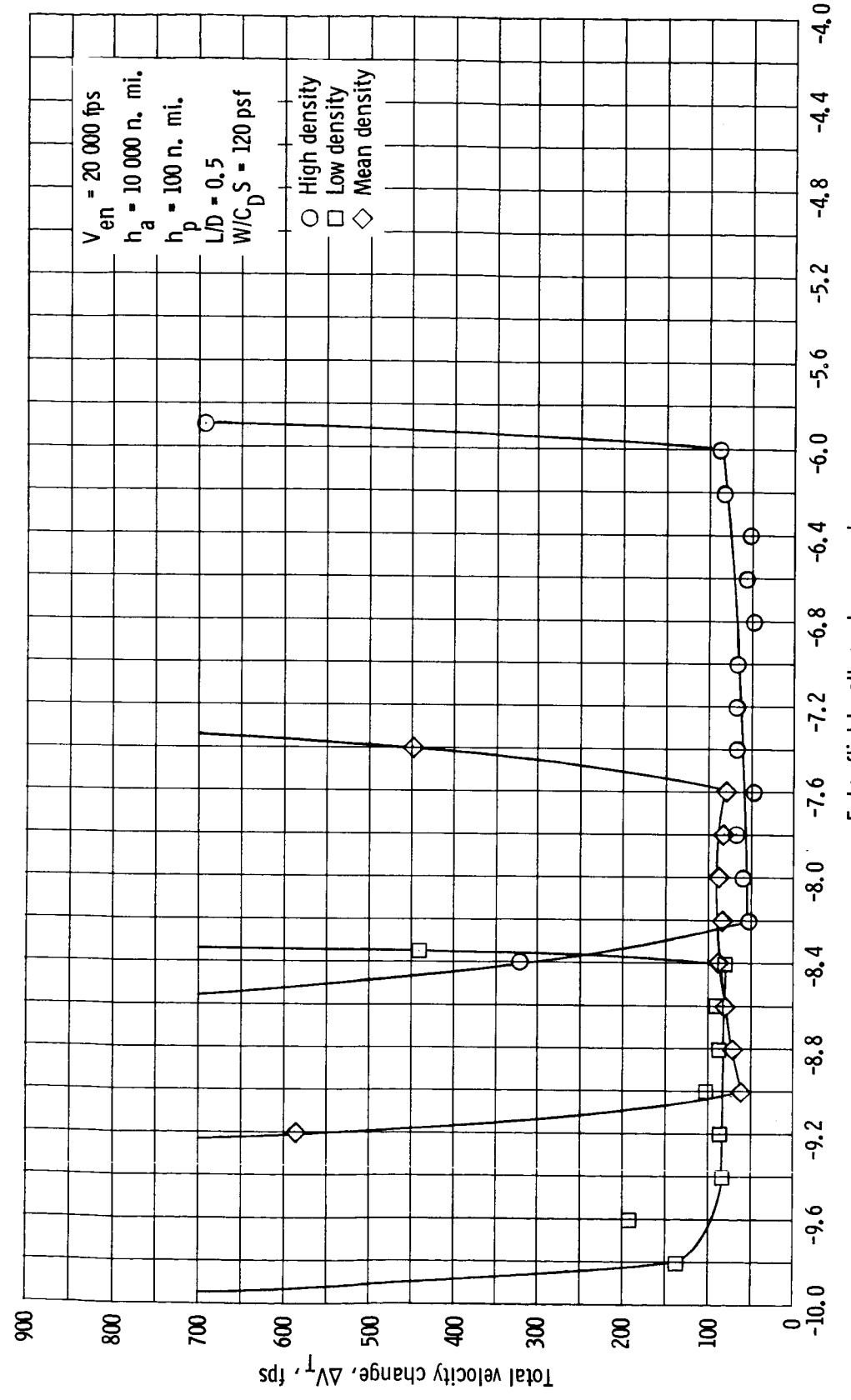

Figure 8. - Total velocity change required to establish target orbit if the guidance is based on correct atmospheric parameters.

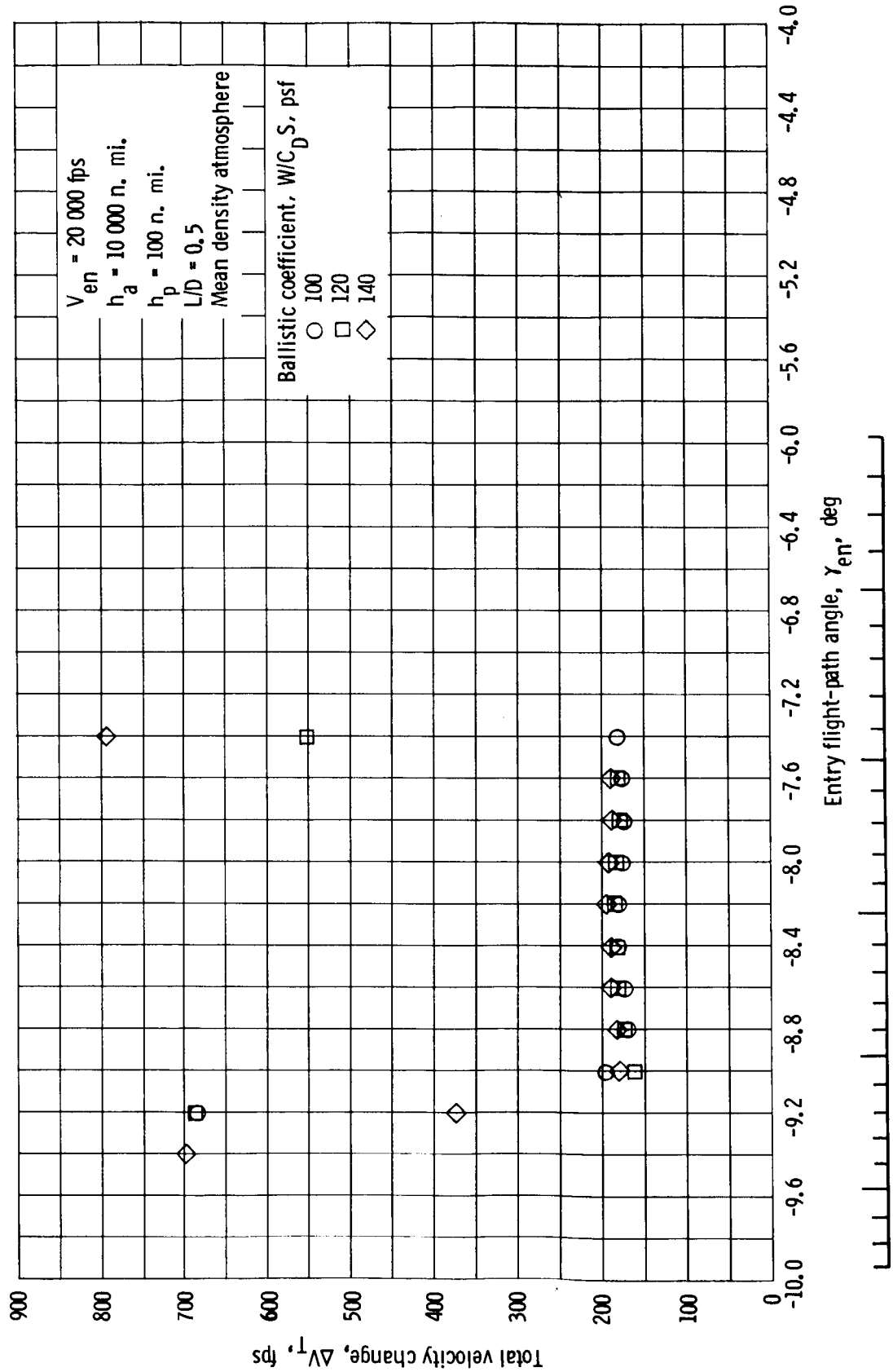

Figure 9. - Effect of variations in ballistic coefficient upon total velocity change.

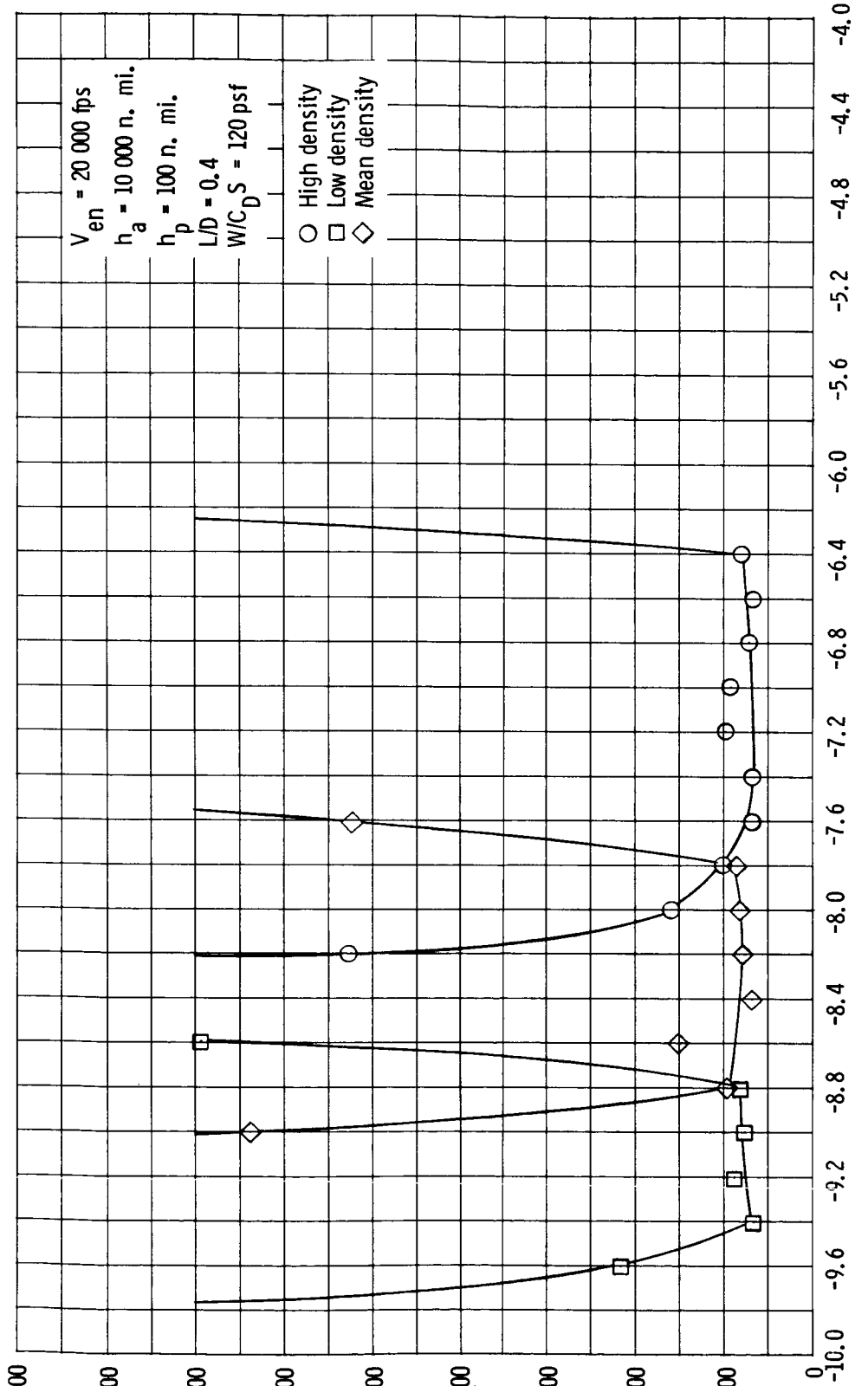

Figure 10. - Effect of reduction in L/D upon total velocity change required to establish target orbit.

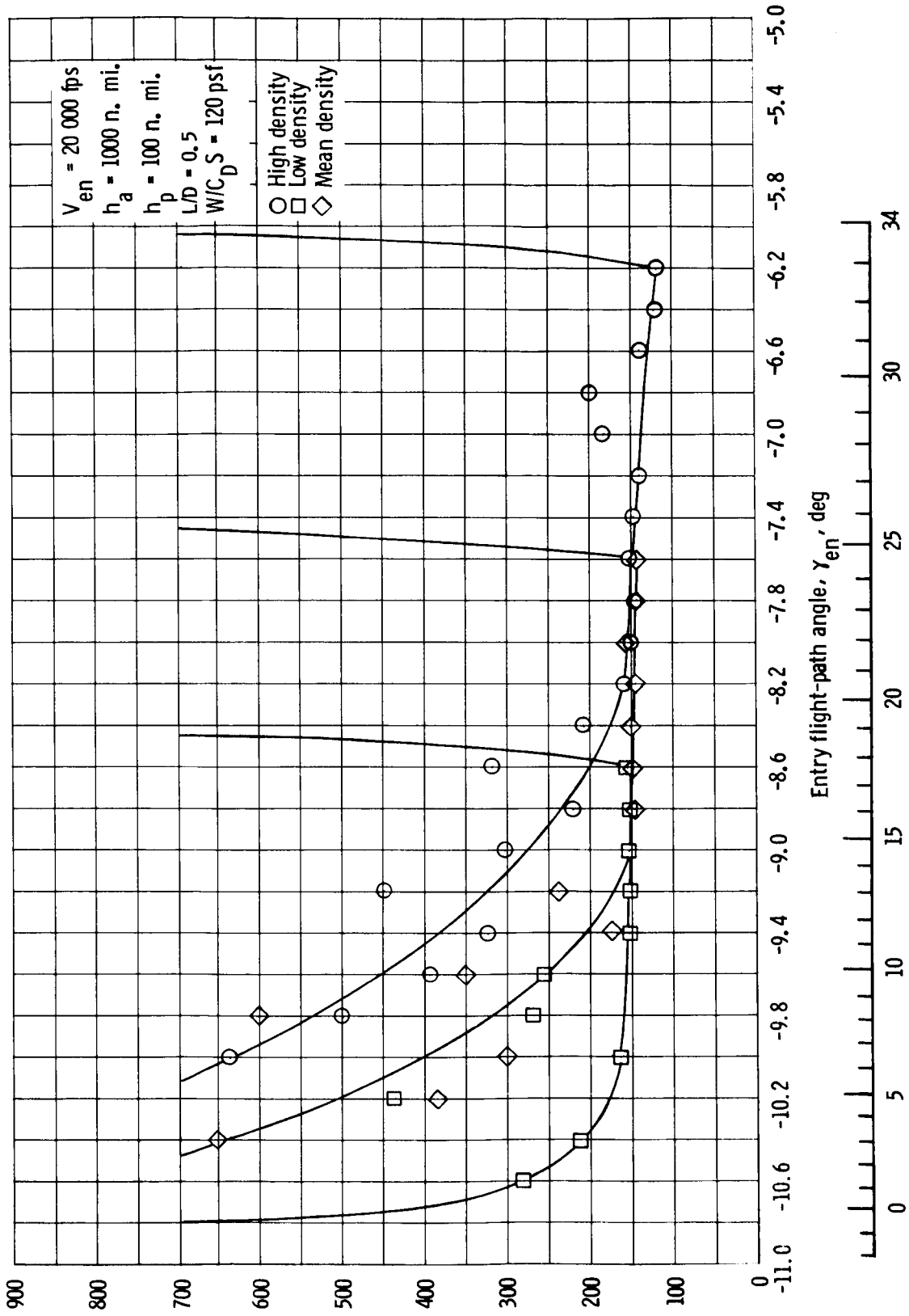

Figure 11.- Total velocity change required to establish target orbit with apoapsis altitude of 1000 nautical miles.

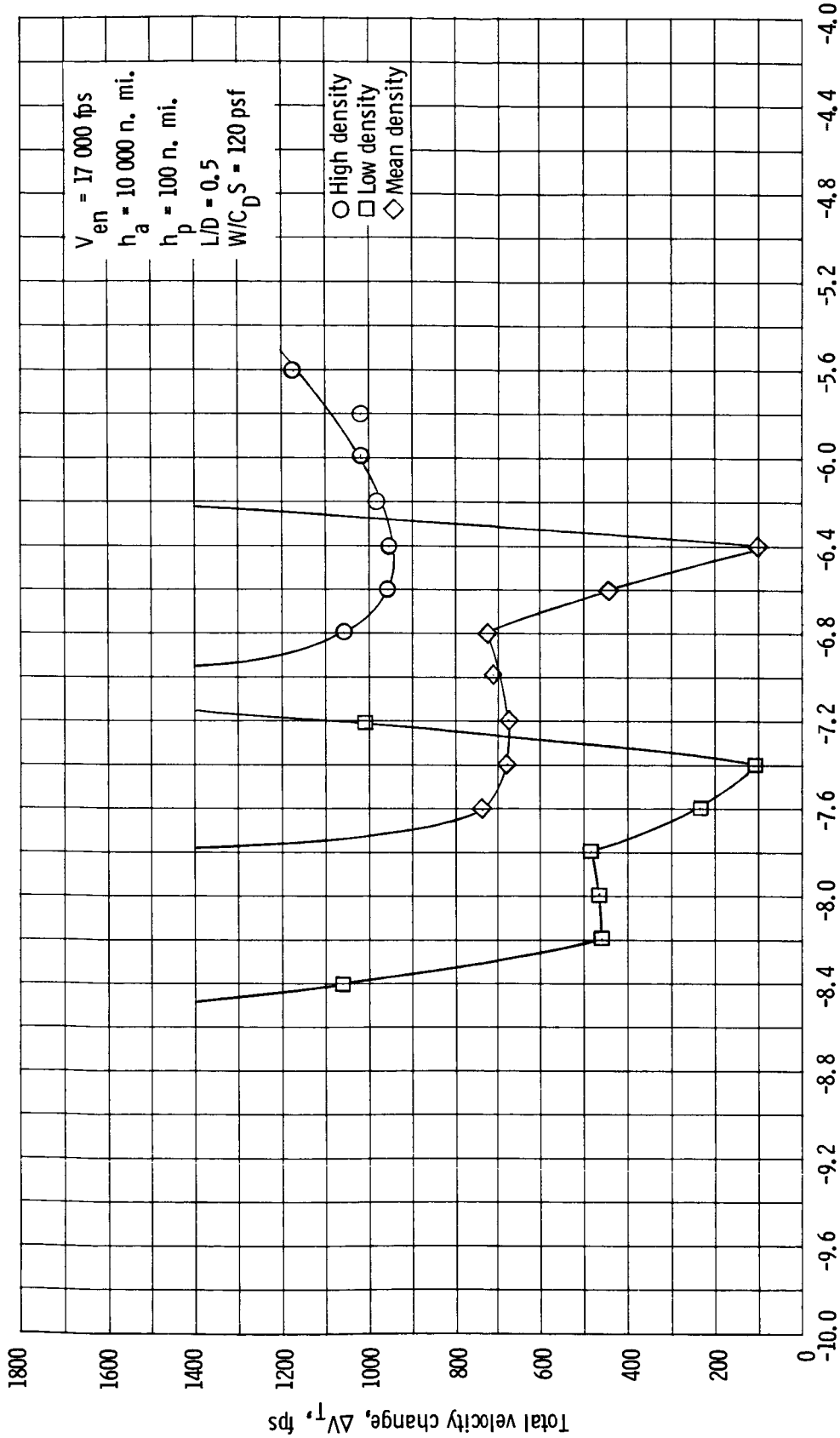

Figure 12.- Total velocity required to achieve target orbit with an apoapsis altitude of 10 000 nautical miles if entry velocity is 17 000 feet per second.

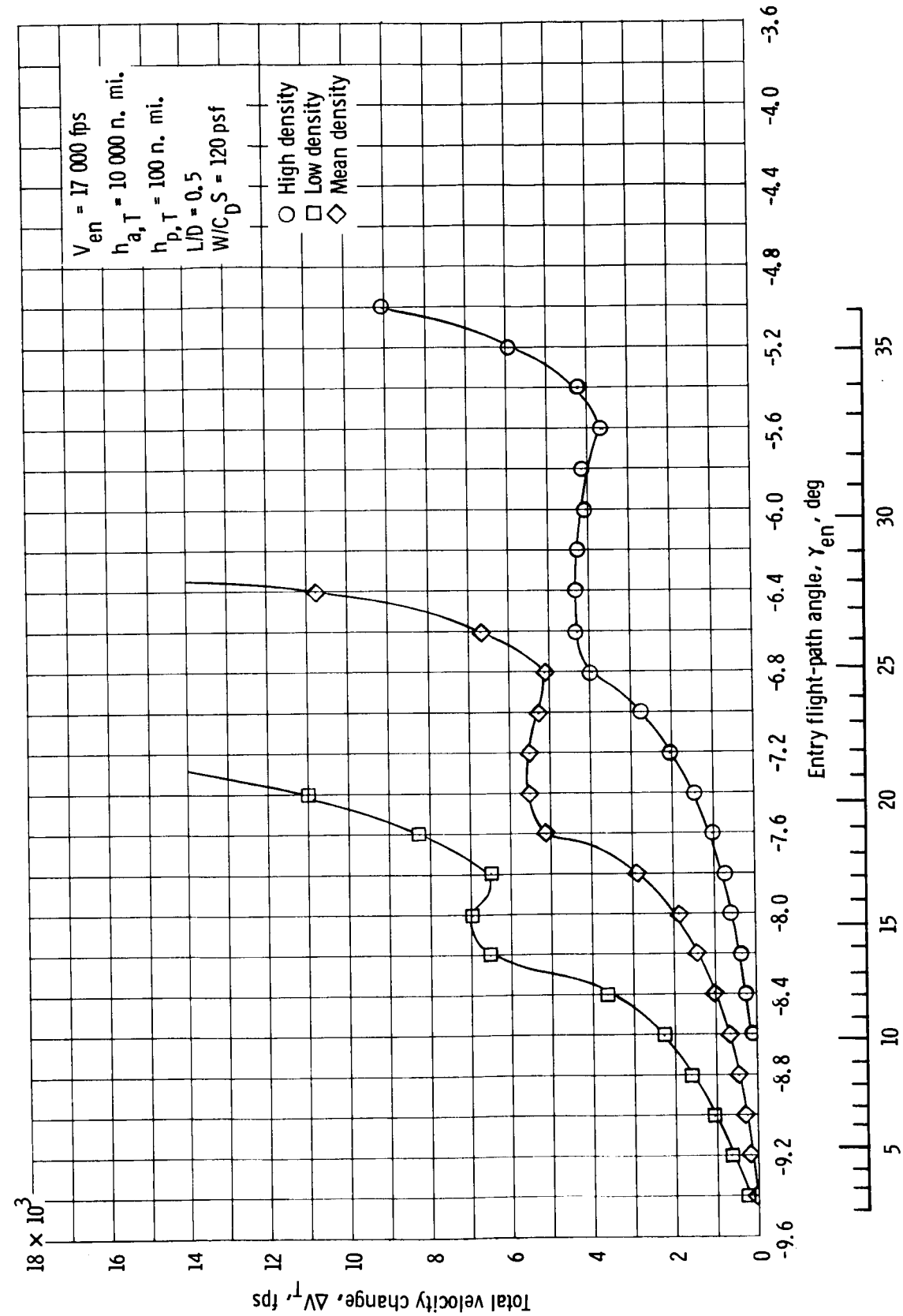

Figure 13.- Apoapsis altitude of exit trajectory if target apoapsis altitude is 10 000 nautical miles and the entry velocity is 17 000 feet per second.

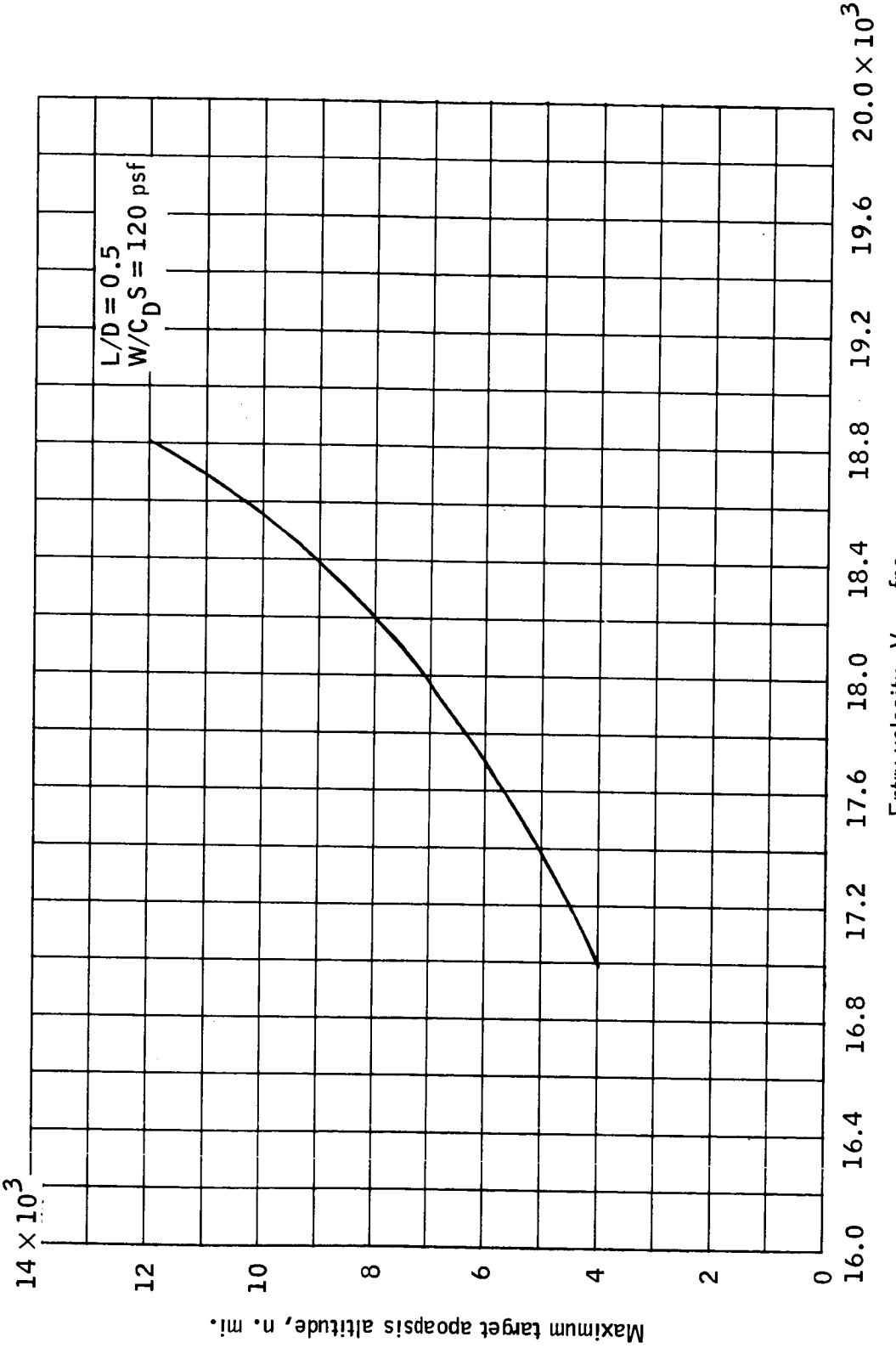

Figure 14.- Maximum target apoapsis altitude.

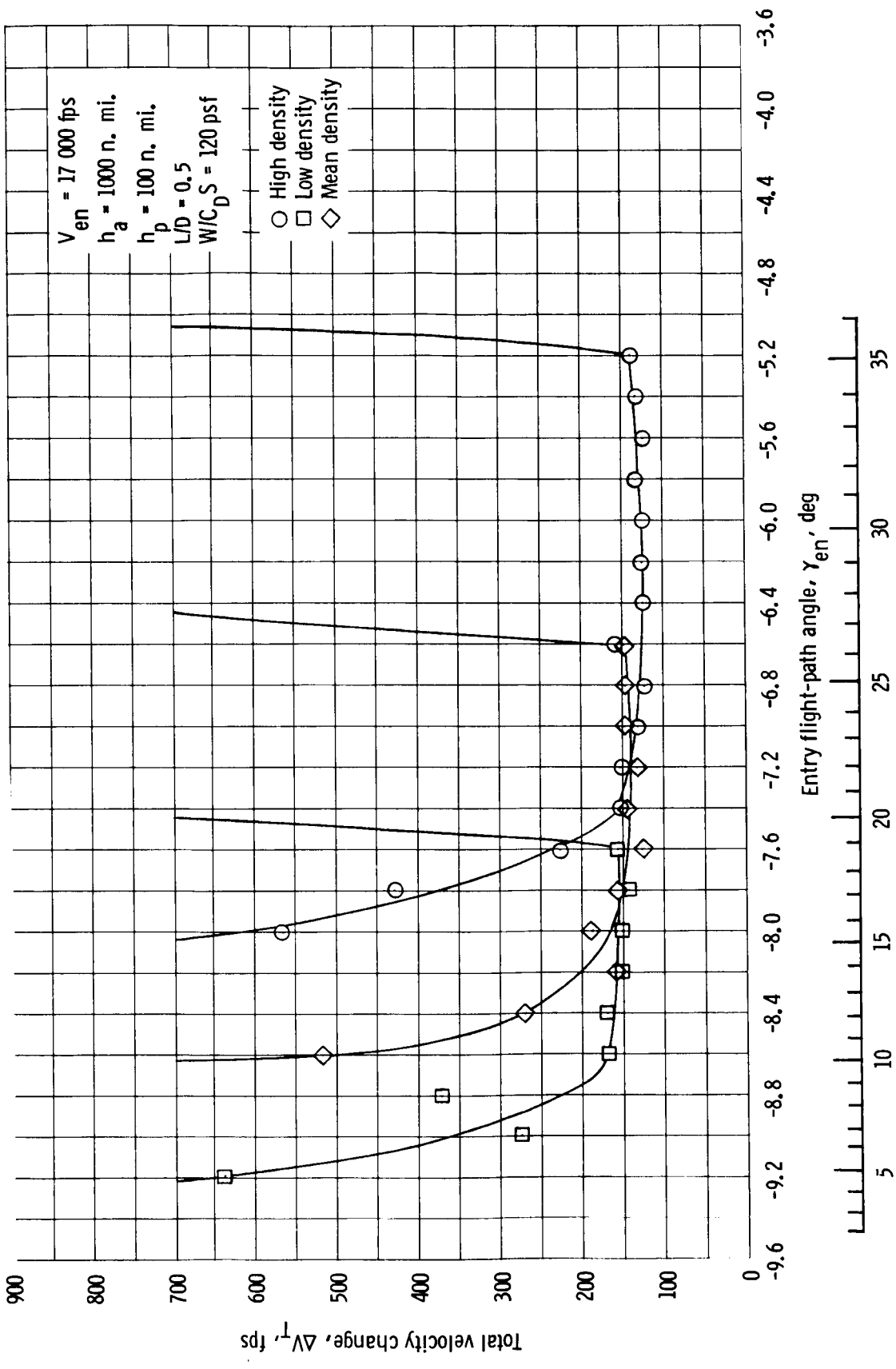

Figure 15.- Effect of decreasing apoapsis altitude to 1000 nautical miles if entry velocity is 17 000 feet per second.

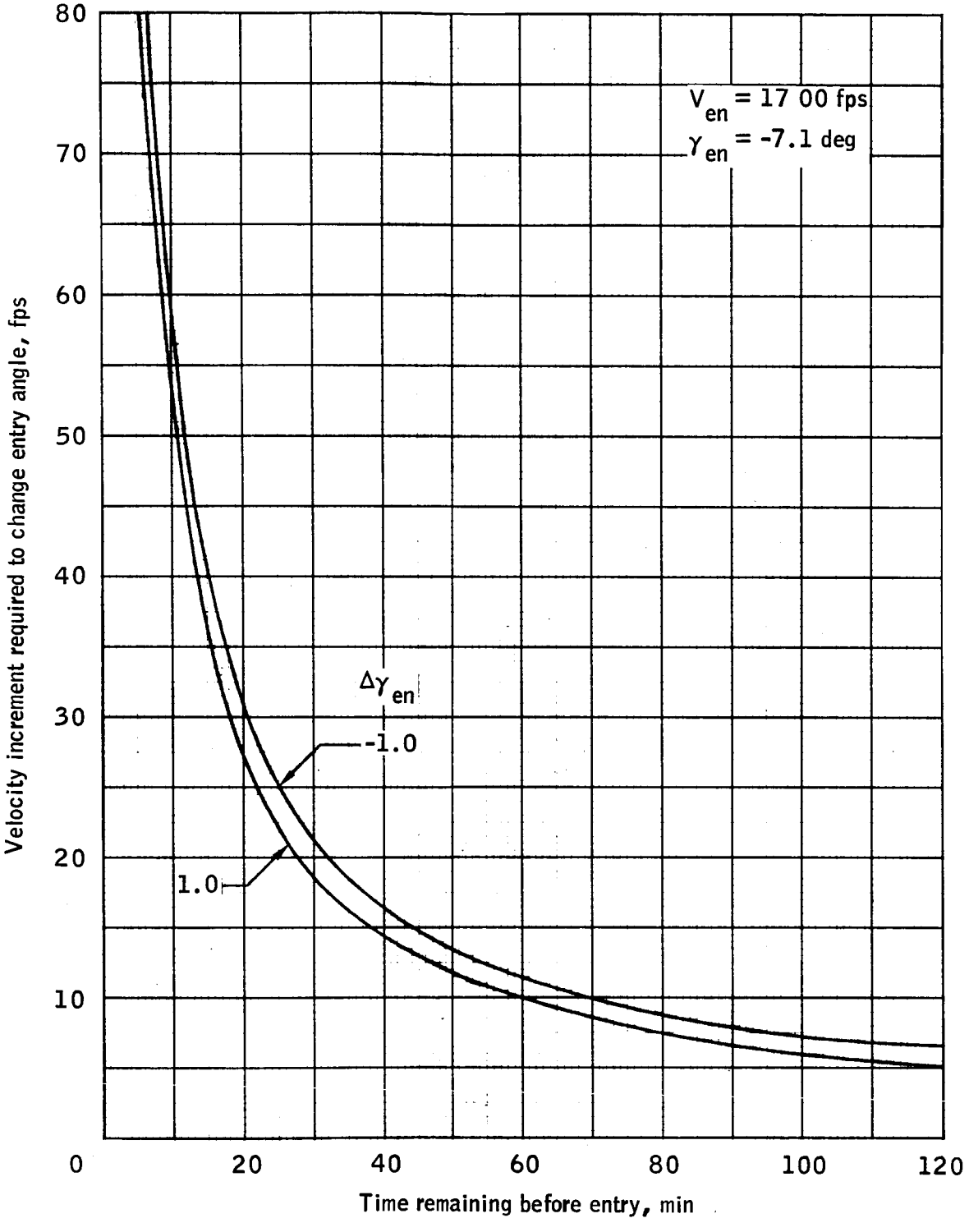

Figure 16.- Velocity increment required to change entry angle as a function of time remaining until entry.

REFERENCES

1. Chapman, Dean R.: An Analysis of the Corridor and Guidance Requirements for Supercircular Entry into Planetary Atmospheres. NASA TR R-55, 1960.

2. Levine, Philip: The Dynamics and Flight Environment of Lifting Vehicles Entering the Atmospheres of Earth, Mars, and Venus. Symposium on Dynamics of Manned Lifting Planetary Entry. Edited by Scala, S. M.; Harrison, A. C.; and Rogers, M. John Wiley and Sons, 1963.

3. Pritchard, E. Brian: Velocity Requirements and Re-Entry Flight Mechanics for Manned Mars Missions. J. Spacecraft and Rockets, Volume 1, No. 6, Nov.-Dec. 1964, pp 605-610.

4. Finch, Thomas W.: Aerodynamic Braking Trajectories for Mars Orbit Attainment. J. Spacecraft and Rockets, Volume 2, No. 4, July-Aug. 1965, pp 497-500.

5. Eggers, Alfred J.; and Swenson, Byron L.: Lifting Entry Vehicles for Future Space Missions. Astronautics and Aeronautics, Volume 5, No. 3, March 1967, pp 24-33.

6. Boobar, M. G.; Repic, E. M.; and McDermont, A. M.: Approach and Entry Corridors for Aerobraking at Mars and Venus. J. Spacecraft and Rockets, Volume 4, No. 5, May 1967, pp 682-684.

7. Knip, Gerald, Jr.; and Zola, Charles L.: Three-Dimensional Trajectory Analysis for Round-Trip Missions to Mars. NASA TN D-1316, Oct. 1962.

8. Taylor, James J.; and McNeely, John T.: Mars Landing Mission Mode Comparison. NASA TM X-1629, Aug. 1968.

9. Repic, E. M.; Boobar, M. G.; and Chapel, F. G.: Aerobraking as a Potential Planetary Capture Mode. J. Spacecraft and Rockets, Volume 5, No. 8, Aug. 1968, pp 921-926.

10. Evans, Dallas E.; Pitts, David E.; and Kraus, Gary L.: Venus and Mars Nominal Environment for Advanced Manned Planetary Mission Programs. NASA SP-3016, Second Edition, 1967.

11. Wingrove, Rodney C.: Trajectory Control Problems in Planetary Entry of Manned Vehicles. J. Spacecraft and Rockets, Volume 2, No. 6, Nov.-Dec. 1965, pp 883-888.

12. Wingrove, R. C.: Survey of Atmospheric Re-Entry Guidance and Control Methods. AIAA Journal, Volume 1, No. 9, Sept. 1963, pp 2019-2029.

13. Funk, Jack; Taylor, James J.; Thibodeau, Joseph R., III; Lowes, Flora B.; and McNeely, John T.: Manned Exploration of Mars: A Minimum-Energy Mission Plan for Maximum Scientific Return. MSC IN 68-FM-70, April 1968.

14. Morth, R.: Reentry Guidance for Apollo. MIT/IL Report R-532, Jan. 1966.

15. White, Jack A.: Feasibility Study of a Bang-Bang Path Control for a Reentry Vehicle. NASA TN D-2049, Nov. 1963.

16. Loh, W. H. T.: Dynamics and Thermodynamics of Planetary Entry. Prentice-Hall, Inc., 1963.

17. Loh, W. H. T.: Extension of the Second-Order Theory of Entry Mechanics to Oscellatory-Type Entry Solutions. AIAA Journal, Volume 3, No. 9, Sept. 1965, pp 1688-1691.

18. Wang, H. E.: Motion of Re-Entry Vehicles During Constant-Altitude Glide. AIAA Journal, Volume 3, No. 7, July 1965, pp 1346-1347.

19. Michaux, C. M.: Handbook of the Physical Properties of the Planet Mars. NASA SP-3030, 1967.

20. Murtagh, T. B.; Lowes, F. B.; and Bond, V. R.: Navigation and Guidance Analysis of a Mars Probe Launched From a Manned Flyby Spacecraft. NASA TN D-4512, 1968.

21. Ehricke, Krafft A.: Space Flight, Volume 1, Environment and Celestial Mechanics. D. Van Nostrand Co., Inc., Princeton, N. J., 1960.